Reversed Lewis Acidity of Mixed Boron Halides: An Infrared Study of the Van der Waals Complexes of BF_xCl_y with CH_3F in Cryosolution

B. J. van der Veken* and E. J. Sluyts

Contribution from the Department of Chemistry, RUCA, Groenenborgerlaan 171, B2020 Antwerpen, Belgium

Received July 16, 1997[⊗]

Abstract: Complexes of mixed boron halides BF_xCl_{3-x} ($x = 1, 2$) with CH_3F have been detected in solutions in liquid argon (86−115 K), using infrared spectroscopy. The spectra of the complexes have been interpreted by using *ab initio* calculations at the MP2/6-31+G** level, and indicate the presence of a conformational equilibrium for both boron halides. For $CH_3F{\cdot}BF_2Cl$ the conformationally averaged $\Delta H°$ was measured to be −12.4(3) kJ mol^{-1}, while for $CH_3F{\cdot}BFCl_2$ it was found to be −10.8(6) kJ mol^{-1} for the C_1 conformer, and −8.6(6) kJ mol^{-1} for the C_s conformer. For solutions containing BCl_3, even at the highest concentrations, no adducts with CH_3F were detected. Combined with existing data on $CH_3F{\cdot}BF_3$, these results show that for weakly bound complexes the Lewis acidity of the boron halides contradicts the established order. This is attributed to the electrostatic nature of the van der Waals bond.

Introduction

The relative Lewis acidity of boron trihalides has been determined from studies of adducts with various Lewis bases, and it is generally accepted that BCl_3 is a stronger Lewis acid than BF_3. The order is imposed by the strength of the π-back-bonding from the halogen to the boron atom, which for fluorine is more important, because the size of its lone pairs allows more efficient overlap with the empty boron p_z orbital.[1]

In a recent theoretical study[2] the accepted order was confirmed for adducts with strong electron donors such as NH_3 or NMe_3. For these, the theoretical results agree with experimental data. However, in the same study it was remarked that for the weakly bound molecules $OC{\cdot}BX_3$ and $MeCN{\cdot}BX_3$ the stability of the BCl_3 adduct is calculated to be lower than that of the BF_3 adduct, i.e., for the weakly bound adducts BCl_3 is the *weaker* Lewis acid. Unfortunately, no experimental data were produced to substantiate the calculation. Whatever the order of Lewis acidity, it seems reasonable to expect that in the series BF_xCl_{3-x}, with x varying from 3 to 0, there will be a gradual change in acidity. Thus, a study of weak adducts of mixed boron halides could provide evidence for a reversed acidity order.

Recently, we have studied,[3] using infrared spectroscopy of cryosolutions, the complex between CH_3F and BF_3, and the complexation enthalpy in liquid argon was found to be −16.8(5) kJ mol^{-1}. This value puts the adduct in the realm of weakly bound van der Waals molecules. By using the same techniques, complexation enthalpies as low as 3−4 kJ mol^{-1} have been measured,[4] showing that the technique has sufficient dynamical range to prove an eventual reversed order for CH_3F adducts. Therefore, this Lewis base was selected for our investigation.

Peripheral to the above, there is a second theme to this investigation. Analogous to the structure of $HF{\cdot}BF_3$, which was established from microwave spectroscopy,[5] the *ab initio* calculations on $CH_3F{\cdot}BF_3$ show that the C−F···B angle equals 118°, resulting in a complex with C_s symmetry. A similar complex with a mixed halide BX_2Y can give rise to two different conformers. The more symmetric of these has a symmetry plane containing the C, F, B, and Y atoms, while the other conformer has C_1 symmetry. The present boron halides are of this type, and it was judged interesting to investigate if a conformational equilibrium can be detected.

In the paragraphs below we will discuss the infrared spectra and the stability of the complexes observed in liquid argon. The results of *ab initio* calculations on the complexes will be used to interpret the vibrational spectra, and evidence for conformational equilibria in the complex with BF_2Cl and $BFCl_2$ will be presented. Also, it will be shown that the complexation enthalpy decreases with increasing chlorination of the boron halide, confirming a reversed acidity order for weakly bound complexes.

Experimental Section

The mixed boron halides were prepared as descirbed by Lindeman et al.,[6] i.e. by mixing BF_3 and BCl_3 in the vapor phase, at room temperature. The rapid equilibration results in a mixture containing BF_3, BF_2Cl, $BFCl_2$, and BCl_3. The fractions of BF_2Cl and $BFCl_2$ can be altered by varying the relative amounts of BF_3 and BCl_3, which proved helpfull in the assignment of the spectra. BF_3 and BCl_3 were provided by Praxair, and were used without further purification. In the spectra of mixed boron halides, HCl was observed as an impurity, due to hydrolysis of some of the BCl_3. No boron-containing hydrolysis products could be detected in the spectra, presumably because they precipitated on the walls of the filling manifold and cell.

The cryosolution setup consists of a 4-cm copper cell, equipped with wedged silicon windows, which is suspended in a vacuum shroud. The cell is cooled with boiling liquid nitrogen and is connected to a manifold for filling and evacuation. Solutions were prepared by first condensing the monomers in the cooled cell, followed by condensation, using bursts

⊗ Abstract published in *Advance ACS Abstracts,* November 1, 1997.

(1) Shriver, D. F.; Atkins, P. W.; Langford, C. H. *Inorganic Chemistry*, 2nd ed.; Oxford University Press: Oxford, 1994; p 205.

(2) Jonas, V.; Frenking, G.; Reetz, M. T. J. *Am. Chem. Soc.* **1994**, *116*, 8741.

(3) Van der Veken, B. J.; Sluyts, E. J. *J. Phys. Chem.* Submitted for publication.

(4) Van der Veken, B. J.; De Munck, F. R. *J. Chem. Phys.* **1992**, *97*, 3060.

(5) Phillips, J. A.; Canagaratna, M.; Goodfriend, H.; Grushow, A.; Almlöf, J.; Leopold, K. R. *J. Am. Chem. Soc.* **1995**, *117*, 12549.

(6) Lindeman, L. P.; Wilson, M. K. *J. Chem. Phys.*, **1956**, *24*, 242.

S0002-7863(97)02385-8 CCC: $14.00

Table 1. *Ab Initio* Complexation Energies, ΔE, and van der Waals Bond Lengths, R_{vdW}, for CH_3F Complexes of Mixed Boron Halides

complex	ΔE/kJ mol^{-1}	R_{vdW}/Å
$CH_3F{\cdot}BF_3$	−25.97[a]	2.2635[a]
$CH_3F{\cdot}BF_2Cl$ (C_s)	−23.13	2.3719
$CH_3F{\cdot}BF_2Cl$ (C_1)	−22.65	2.3801
$CH_3F{\cdot}BFCl_2$ (C_1)	−21.25	2.4885
$CH_3F{\cdot}BFCl_2$ (C_s)	−19.51	2.4965
$CH_3F{\cdot}BCl_3$	−19.79	2.5942

[a] Taken from ref 3.

of pressurized gas, of the solvent gas argon. The latter process causes strong turbulence, so that no extra mixing is required. The argon was provided by L'Air Liquide, and had a stated purity of 99.9999%.

Infrared spectra were recorded on Bruker IFS 113v and IFS 66v spectrometers, using a globar source, a Ge/KBr beam splitter, and a broad band MCT detector. For each spectrum 200 interferograms were averaged, Happ Genzel apodized, and Fourier transformed with a zero filling of 4 to produce a spectrum with a resolution of 0.5 cm^{-1}.

Ab initio calculations were carried out with the Gaussian 94 programs,[7] at the MP2/6-31+G** level. Berny optimization with tight convergence was used, and the correlation was calculated with use of all molecular orbitals. The vibrational spectra were calculated by using the analytical (number of basis functions ≤120) or numerical (number of basis functions >120) second derivatives from the analytically determined Cartesian first derivatives of the energy.

Results

The *ab initio* calculations on the adducts of CH_3F with BF_2Cl, $BFCl_2$, and BCl_3 all result in a converged structure similar to that of $CH_3F{\cdot}BF_3$. Thus, a van der Waals bond is formed between the (C)F atom and the boron atom. The C−F bond shows an angle with the van der Waals bond between 115° and 125°, depending on species and conformation. For BF_2Cl and $BFCl_2$ two different stable conformers, with slightly different energies, occur. In one of these, the C−F bond is staggered between the two similar substituents on the boron atom, and has C_s symmetry. The other has its C−F bond staggered between two disimilar boron susbstituents and has C_1 symmetry. In Table 1 we give the complexation energy, defined as the energy of the complex from which the monomer energies have been subtracted, and the van der Waals bond length for the various complexes. For comparison, the previously published data[3] on $CH_3F{\cdot}BF_3$ are also given. For all the complexes the van der Waals bond is formed between the same two atoms. Therefore, its length is a measure of the strength of the complex.[2] It can be seen in Table 1 that the bond length steadily increases from the BF_3 to the BCl_3 complex, i.e. the van der Waals bond becomes weaker. This fully agrees with the results of Jonas et al.[2] on similar weak complexes. The calculated complexation energies display the same trend, except for the C_s conformer of $CH_3F{\cdot}BFCl_2$, which is calculated to be marginally more stable than the BCl_3 complex. The reason for this discrepancy is not clear.

In Tables 2−5, selected calculated vibrational frequencies and infrared intensities of the complexes are collected. For brevity, we have included only the transitions with sufficient intensity that fall in the spectral range studied. Also given are the complexation shifts, defined as the difference between the frequencies in complex and in monomer.

The solutions studied contain a variety of monomers; their spectra in liquid Ar (CH_3F, BF_3),[8−10] in solid argon (BF_2Cl, $BFCl_2$, BCl_3),[11] or in the vapor phase[6] have been described before. The frequencies observed for the latter species in liquid argon (LAr) are very close to those observed in the other phases. For instance, the frequencies are typically between 1 and 5 cm^{-1} higher in LAr than in solid argon. Their assignment, by comparing to the previous studies, is straightforward. Therefore, we will not list the monomer frequencies.

Because of the weak interaction between the monomers, the vibrations of the complex can be divided in modes localized in the monomers, and in intermolecular modes. The latter have low frequencies and have not been observed in the present study. The former can unambiguously be correlated with the modes of the isolated monomers. Therefore, we will describe such complex modes starting from the symbol of the corresponding monomer mode. For the latter, the standard numbering scheme is used,[6] and the formula of the monomer is given as a superscript. Where necessary, this symbol is followed by the chemical formula of the complex, in brackets. Where no isotopic species is indicated in the formula, it is assumed that the different isotopes appear accidentally degenerate.

The behavior of mixtures of CH_3F and the boron halides in liquid argon is exemplified in Figure 1. The bottom spectrum was taken from a solution containing only the boron halides. The bands at 1346 and 1303 cm^{-1} are the ν_1, i.e. the B−F stretch, of $^{10}BFCl_2$ and $^{11}BFCl_2$, respectively, and the bands at 1277 and 1234 cm^{-1} are the $^{10}B/^{11}B$ isotopic doublet of ν_1, i.e. the symmetric BF_2 stretch, of BF_2Cl. The *ab initio* intensity for ν_1^{BF2Cl} is approximately 50% higher than that for ν_1^{BFCl2}, so that the spectrum shows that the solution contained similar concentrations of BF_2Cl and $BFCl_2$. Figure 1b gives the spectrum after adding CH_3F to the solution. New bands are observed near 1260 and 1219 cm^{-1}. At the lowest temperatures, these bands have a clear doublet structure. Their relative intensity suggests they arise in a ^{10}B and a ^{11}B compound, respectively. In the same spectral region, ν_1^{BF2Cl} and ν_1^{BFCl2} occur, and it appears logical to associate the new bands with either $CH_3F{\cdot}BF_2Cl$ or $CH_3F{\cdot}BFCl_2$. The *ab initio* calculations predict a downward complexation shift for ν_1^{BF2Cl} of 18 and 11 cm^{-1} for the C_1 and C_s conformer, respectively, while ν_1^{BFCl2} shifts upward by 9 cm^{-1} for the C_s conformer and downward by 17 cm^{-1} for the C_1 conformer. The new bands in Figure 1 occur downward of the respective isotopic ν_1^{BF2Cl}, by 17 and 14 cm^{-1}, while their shifts with respect to the ν_1^{BFCl2} are inconsistent with the predictions for $CH_3F{\cdot}BFCl_2$. Therefore, we assign these bands to ν_1^{BF2Cl} ($CH_3F{\cdot}BF_2Cl$). The doublet structure of these bands is a strong indication for the presence of a conformational equilibrium, and we assign the components of the doublets in agreement with the *ab initio* predictions. It is also clear that in Figure 1b, near ν_1^{BFCl2} no new bands can be distinguished. The spectrum obtained from a solution to which nearly the 10-fold amount of CH_3F was added is shown in Figure 1c. It can be seen that the region of ν_1^{BF2Cl} is now strongly dominated by the complex bands, showing that in the solution most of the BF_2Cl has been transformed into adduct with CH_3F. At the same time, new bands occur near ν_1^{BFCl2}.

(7) *Gaussian 94*, Revision B.2; Frisch, M. J.; Trucks G. W.; Schlegel, H. B.; Gill, P. M. W.; Johnson, B. G.; Robb, M. A.; Cheeseman, J. R.; Keith, T.; Petersson, G. A.; Montgomery, J. A.; Raghavachari, K.; Al-Laham, M. A.; Zakrzewski, V. G.; Ortiz, J. V.; Foresman, J. B.; Cioslowski, J.; Stefanov, B. B.; Nanayakkara, A.; Challacombe, M.; Peng, C. Y.; Ayala, P. Y.; Chen, W.; Wong, M. W.; Andres, J. L.; Replogle, E. S.; Gomperts, R.; Martin, R. L.; Fox, D. J.; Binkley, J. S.; Defrees, D. J.; Baker, J.; Stewart, J. P.; Head-Gordon, M.; Gonzalez, C.; and Pople, J. A.; Gaussian, Inc.: Pittsburgh, PA, 1995.

(8) Sluyts, E. J.; Van der Veken, B. J. *J. Am. Chem. Soc.* **1996**, *118*, 440.

(9) Kolomiitsova, T. D.; Milke, Z.; Tokhadze, K. G.; Schepkin, D. N. *Opt. Spectrosc. (USSR)* **1979**, *46*, 391.

(10) Barri, M. F.; Tokhadze, K. G. *Opt. Spectrosc. (USSR)* **1981**, *51*, 70.

(11) Maier, W. B., II; Holland, R. F. *J. Chem. Phys.* **1980**, *72*, 6661.

Table 2. *Ab Initio* Frequencies, Infrared Intensities, and Complexation Shifts for Selected Vibrational Modes of the C_s Conformer of $CH_3F{\cdot}BF_2Cl$

	$CH_3F{\cdot}{}^{10}BF_2{}^{35}Cl$		$CH_3F{\cdot}{}^{10}BF_2{}^{37}Cl$		$CH_3F{\cdot}{}^{11}BF_2{}^{35}Cl$		$CH_3F{\cdot}{}^{11}BF_2{}^{37}Cl$	
	ν (Int)	$\Delta\nu$	ν (Int)	$\Delta\nu$	ν (Int)	$\Delta\nu$	ν (Int)	$\Delta\nu$
$\nu_{4a}(CH_3F)$	3285.0 (14)	21.3	3285.0 (14)	21.3	3285.0 (14)	21.3	3285.0 (14)	21.3
$\nu_{4b}(CH_3F)$	3283.8 (12)	20.1	3283.8 (12)	20.1	3283.8 (12)	20.1	3283.8 (12)	20.1
$\nu_1(CH_3F)$	3159.0 (27)	12.5	3159.0 (27)	12.5	3159.0 (27)	12.5	3159.0 (27)	12.5
$\nu_4(BF_2Cl)$	1430.8 (367)	−28.3	1430.8 (367)	−28.3	1381.2 (340)	−27.3	1381.2 (340)	−27.3
$\nu_1(BF_2Cl)$	1282.1 (583)	−10.8	1281.1 (581)	−10.9	1237.2 (534)	−10.9	1236.2 (532)	−11.0
$\nu_3(CH_3F)$	1028.9 (116)	−30.5	1028.9 (116)	−30.5	1028.7 (116)	−30.7	1028.7 (116)	−30.7
$\nu_2(BF_2Cl)$	705.9 (34)	−5.6	702.1 (34)	−5.4	701.9 (35)	−5.7	698.0 (35)	−5.4
$\nu_6(BF_2Cl)$	580.8 (140)	−53.3	580.4 (139)	(−53.4)	559.1 (128)	−49.7	558.8 (128)	−49.7

Table 3. *Ab Initio* Frequencies, Infrared Intensities, and Complexation Shifts for Selected Vibrational Modes of the C_1 Conformer of $CH_3F{\cdot}BF_2Cl$

	$CH_3F{\cdot}{}^{10}BF_2{}^{35}Cl$		$CH_3F{\cdot}{}^{10}BF_2{}^{37}Cl$		$CH_3F{\cdot}{}^{11}BF_2{}^{35}Cl$		$CH_3F{\cdot}{}^{11}BF_2{}^{37}Cl$	
	ν (Int)	$\Delta\nu$	ν (Int)	$\Delta\nu$	ν (Int)	$\Delta\nu$	ν (Int)	$\Delta\nu$
$\nu_{4a}(CH_3F)$	3286.0 (12)	22.3	3286.0 (12)	22.3	3286.0 (12)	22.3	3286.0 (12)	22.3
$\nu_{4b}(CH_3F)$	3281.6 (15)	17.9	3281.6 (15)	17.9	3281.6 (15)	17.9	3281.6 (14)	17.9
$\nu_1(CH_3F)$	3158.8 (26)	12.3	3158.8 (26)	12.3	3158.8 (26)	12.3	3158.8 (26)	12.3
$\nu_4(BF_2Cl)$	1449.9 (372)	−9.2	1449.9 (372)	−9.2	1399.7 (349)	−8.8	1399.7 (349)	−8.8
$\nu_1(BF_2Cl)$	1274.0 (559)	−18.9	1273.1 (558)	−18.9	1230.0 (503)	−18.1	1229.1 (501)	−18.1
$\nu_3(CH_3F)$	1030.3 (114)	−29.1	1030.3 (114)	−29.1	1030.1 (115)	−29.3	1030.1 (115)	−29.3
$\nu_2(BF_2Cl)$	702.4 (31)	−9.1	698.6 (32)	−8.9	698.2 (32)	−9.4	694.2 (33)	−9.2
$\nu_6(BF_2Cl)$	581.7 (143)	−52.4	581.3 (143)	−52.5	559.8 (131)	−49.0	559.5 (130)	−49.0

Table 4. *Ab initio* Frequencies, Infrared Intensities, and Complexation Shifts for Selected Vibrational Modes of the C_1 Conformer of $CH_3F{\cdot}BFCl_2$

	$CH_3F{\cdot}{}^{10}BF^{35}Cl_2$		$CH_3F{\cdot}{}^{10}BF^{35}Cl^{37}Cl$		$CH_3F{\cdot}{}^{11}BF^{35}Cl_2$		$CH_3F{\cdot}{}^{11}BF^{35}Cl^{37}Cl$	
	ν (Int)	$\Delta\nu$	ν (Int)	$\Delta\nu$	ν (Int)	$\Delta\nu$	ν (Int)	$\Delta\nu$
$\nu_{4a}(CH_3F)$	3280.6 (1)	16.9	3280.6 (14)	16.9	3280.6 (14)	16.9	3280.6 (14)	16.9
$\nu_{4b}(CH_3F)$	3278.2 (15)	14.5	3278.2 (15)	14.5	3278.2 (15)	14.5	3278.2 (15)	14.5
$\nu_1(CH_3F)$	3155.9 (28)	9.4	3155.9 (28)	9.4	3155.9 (28)	9.4	3155.9 (28)	9.4
$\nu_1(BFCl_2)$	1326.8 (365)	−17.2	1326.6 (364)	−17.2	1282.2 (338)	−16.8	1282.0 (338)	−16.9
$\nu_4(BFCl_2)$	1083.6 (575)	−8.3	1081.8 (574)	−8.3	1040.9 (550)	−6.9	1039.5 (528)	−6.4
$\nu_3(CH_3F)$	1035.0 (109)	−24.4	1035.0 (108)	−24.4	1033.8 (88)	−25.6	1033.4 (109)	−26.0
$\nu_2(BFCl_2)$	578.7 (8)	−4.7	574.5 (8)	−4.4	576.2 (7)	−5.0	571.9 (7)	−4.8
$\nu_6(BFCl_2)$	515.6 (68)	−39.2	515.1 (68)	−39.3	495.6 (63)	−36.6	495.1 (63)	−36.7

Table 5. *Ab Initio* Frequencies, Infrared Intensities, and Complexation Shifts for Selected Vibrational Modes of the C_s Conformer of $CH_3F{\cdot}BFCl_2$

	$CH_3F{\cdot}{}^{10}BF^{35}Cl_2$		$CH_3F{\cdot}{}^{10}BF^{35}Cl^{37}Cl$		$CH_3F{\cdot}{}^{11}BF^{35}Cl_2$		$CH_3F{\cdot}{}^{11}BF^{35}Cl^{37}Cl$	
	ν (Int)	$\Delta\nu$	ν (Int)	$\Delta\nu$	ν (Int)	$\Delta\nu$	ν (Int)	$\Delta\nu$
$\nu_{4a}(CH_3F)$	3279.0 (17)	15.3	3279.0 (17)	15.3	3279.0 (17)	15.3	3279.0 (17)	15.3
$\nu_{4b}(CH_3F)$	3276.8 (14)	13.1	3276.8 (14)	13.1	3276.8 (14)	13.1	3276.8 (14)	13.1
$\nu_1(CH_3F)$	3154.8 (26)	8.3	3154.8 (26)	8.3	3154.8 (26)	8.3	3154.8 (26)	8.3
$\nu_1(BFCl_2)$	1353.1 (366)	9.1	1353.0 (366)	9.2	1307.8 (341)	8.8	1307.7 (340)	8.8
$\nu_4(BFCl_2)$	1069.6 (549)	−22.3	1067.9 (548)	−22.2	1026.3 (504)	−21.5	1024.5 (502)	−21.4
$\nu_3(CH_3F)$	1036.9 (113)	−22.5	1036.9 (113)	−22.5	1036.8 (113)	−22.6	1036.8 (113)	−22.6
$\nu_2(BFCl_2)$	576.3 (7)	−7.1	572.0 (7)	−6.9	573.7 (6)	−7.5	569.3 (6)	−7.4
$\nu_6(BFCl_2)$	514.5 (70)	−40.3	514.1 (70)	−40.3	494.5 (65)	−37.7	494.1 (65)	−37.7

For each isotopomer, one new band appears blue shifted, by approximately 4 cm^{-1}, from the monomer, and the other appears red shifted by 8 cm^{-1}. The directions of the shifts are as predicted for the C_s and C_1 conformers of $CH_3F{\cdot}BFCl_2$, and the shifts show the correct relative magnitude. Therefore, these bands are assigned accordingly. Thus, also for $BFCl_2$ a complex, giving rise to conformational splitting, is observed. The complex bands are much weaker than those of $CH_3F{\cdot}BF_2Cl$ in the same spectrum, while it was argued above that the concentrations of BF_2Cl and $BFCl_2$ are similar. The *ab initio* intensities for the modes involved are of the same magnitude, so that the relative intensities suggest that $CH_3F{\cdot}BFCl_2$ is a weaker complex than $CH_3F{\cdot}BF_2Cl$. This will be confirmed by the temperature study, to be discussed below.

The *ab initio* calculations, Tables 2−5, also predict that in other regions of the spectra complex bands can be expected. This is indeed the case, as illustrated by Figures 2 and 3. The spectrum in Figure 2a was recorded from the same solution as for Figure 1c, while the solution for Figure 2b was the same as for Figure 1b. Figure 2a is dominated by bands of monomer CH_3F, which was present in substantial excess. Nevertheless, shoulders due to a complex are visible on the high-frequency side of ν_1^{CH3F}, $\nu_4{}^{CH3F}$, and $2\nu_1^{CH3F}$. The complex bands dominate the spectrum in Figure 2b, allowing accurate measurement of the shifts, which have been collected in Table 6. This spectrum was recorded from a solution in which no complex bands are detectable near ν_1^{BFCl2} and, thus, the complex bands must be assigned to $CH_3F{\cdot}BF_2Cl$. The complexation shifts of

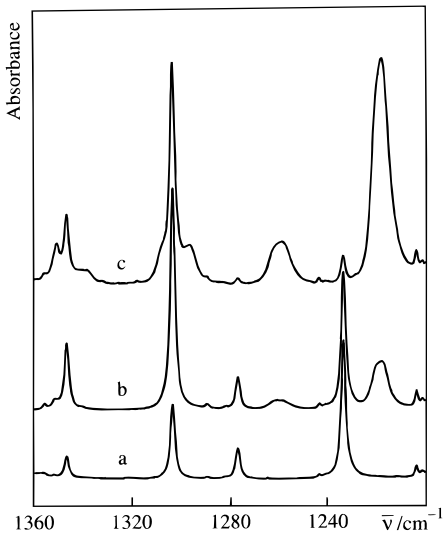

Figure 1. Infrared spectra of solutions in liquid argon at 93 K, in the region of ν_1^{BF2Cl} and ν_1^{BFCl2}: (a) solution containing only the boron trihalides; (b) solution containing the boron trihalides and a small concentration of CH_3F; (c) solution containing the boron trihalides and a large excess of CH_3F.

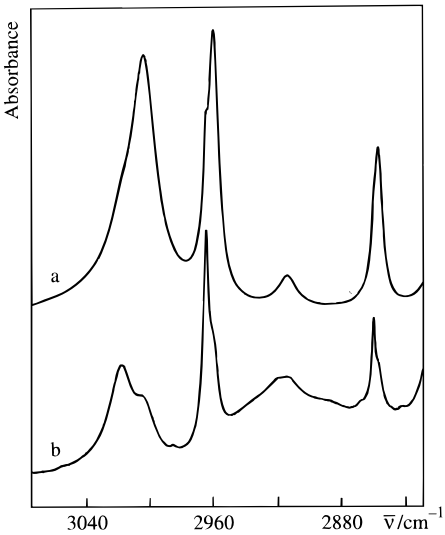

Figure 2. Infrared spectra of solutions in liquid argon at 93 K, in the region of the CH stretches: (a) solution containing the boron trihalides and a large excess of CH_3F; (b) solution containing the boron trihalides and a small concentration of CH_3F.

ν_1^{CH3F} and ν_4^{CH3F} are in the direction predicted, and the shift of ν_4^{CH3F}, 15 cm^{-1}, compares favorably with the predicted value, 20.4 cm^{-1}. The agreement for ν_1^{CH3F} is less good, which, as for $CH_3F{\cdot}BF_3$, is attributed to a small change in the Fermi resonance between ν_1^{CH3F} and $2\nu_2^{CH3F}$ upon complexation. The shifts for the present complex are significantly smaller than those for $CH_3F{\cdot}BF_3$. Assuming that the shifts are related to the strength of the complex, $CH_3F{\cdot}BF_2Cl$ must be the weaker complex. Also this will be confirmed from the temperature study.

Figure 3a gives the region of ν_3^{CH3F}. The triplet near 1025 cm^{-1} is assigned to $\nu_4^{10BFCl2}$, while the bands at 1034 and 1014 cm^{-1} are ν_3^{CH3F} in monomer and complex, respectively. Again, this spectrum was recorded from the same solution as in Figure 1b, from which it follows that the band at 1014 cm^{-1} is due to $CH_3F{\cdot}BF_2Cl$. No conformational or isotopic splitting is observed in this band, which, taking into account its width, is compatible with the *ab initio* predictions. The observed shift

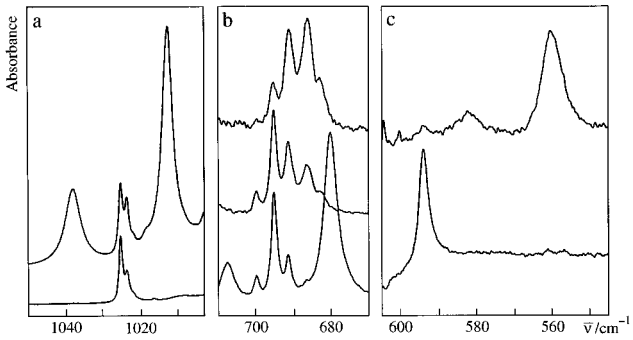

Figure 3. (a) Infrared spectra of solutions in liquid argon at 93 K, in the region of ν_3^{CH3F}: (top) solution containing the boron trihalides and a small concentration of CH_3F; (bottom) solution containing only the boron trihalides. (b) Infrared spectra of solutions in liquid argon at 93 K, in the region of ν_2^{BF2Cl}: (bottom) solution containing only the boron trihalides; (middle) solution containing the boron trihalides and a small concentration of CH_3F; (top) solution containing the boron trihalides and a large excess of CH_3F. (c) Infrared spectra of solutions in liquid argon at 93 K, in the region of ν_6^{BF2Cl}: (bottom) solution containing only the boron trihalides; (top) solution containing the boron trihalides and a large excess of CH_3F.

Table 6. Observed Infrared Frequencies, in cm^{-1}, and Observed and Calculated Complexation Shifts, in cm^{-1}, for $CH_3F{\cdot}BF_2Cl$ and $CH_3F{\cdot}BFCl_2$ in Liquid Argon at 93 K

freq	assignment	$\Delta\nu_{exp}$	$\Delta\nu_{calc}$
3019	ν_4^{CH3F} ($CH_3F{\cdot}BF_2Cl$)	15	20.4[a]
2966	ν_1^{CH3F} ($CH_3F{\cdot}BF_2Cl$)	5	12.3
2861	$2\nu_2^{CH3F}$ ($CH_3F{\cdot}BF_2Cl$)	3	
1350	ν_1^{BFCl2} ($CH_3F{\cdot}{}^{10}BFCl_2$), C_s	4	9.1
1338	ν_1^{BFCl2} ($CH_3F{\cdot}{}^{10}BFCl_2$), C_1	−8	−17.2
1308	ν_1^{BFCl2} ($CH_3F{\cdot}{}^{11}BFCl_2$), C_s	5	8.8
1295	ν_1^{BFCl2} ($CH_3F{\cdot}{}^{11}BFCl_2$), C_1	−8	−16.8
1262	ν_1^{BF2Cl} ($CH_3F{\cdot}{}^{10}BF_2Cl$), C_s	−16	−10.8
1258	ν_1^{BFCl2} ($CH_3F{\cdot}{}^{10}BFCl_2$), C_1	−19	−18.9
1221	ν_1^{BFCl2} ($CH_3F{\cdot}{}^{11}BFCl_2$), C_s	−12	−10.9
1217	ν_1^{BFCl2} ($CH_3F{\cdot}{}^{11}BFCl_2$), C_1	−16	−18.1
1014	ν_3^{CH3F} ($CH_3F{\cdot}BF_2Cl$)	−25	−29.9
691 686 682	ν_2^{BF2Cl} ($CH_3F{\cdot}BF_2Cl$)	−4[b]	−5.6/−9.1
587	ν_6^{BF2Cl} ($CH_3F{\cdot}{}^{10}BF_2Cl$)	−33	−52.8[c]
560	ν_6^{BF2Cl} ($CH_3F{\cdot}{}^{11}BF_2Cl$)	−34	−49.4[c]

[a] Averaged over conformers and boron isotopes. [b] See text. [c] Averaged over conformers.

is −25 cm^{-1}, in the direction predicted by, and in very reasonable agreement with, the calculations. The shift is smaller than that for $CH_3F{\cdot}BF_3$, again suggesting $CH_3F{\cdot}BF_2Cl$ is the weaker complex.

Somewhat more complicated is the region of ν_2^{BF2Cl} shown in Figure 3b. The bottom spectrum was recorded from a solution containing only the boron halides. The broad bands at 709 and 682 cm^{-1} are the $^{10}B/^{11}B$ doublet of ν_2^{BF3}. These bands are absent in the spectra of the mixture: this is a consequence of the limited solubility[3] of $CH_3F{\cdot}BF_3$, which at the temperature used precipitates on the cell walls. It is clear that the amount of CH_3F added to the solution was high enough to quantitatively precipitate the BF_3. The sharper triplet, centered at 695 cm^{-1}, is assigned to BF_2Cl. The 700-cm^{-1} high-frequency component is due to $^{10}BF_2{}^{35}Cl$, the central band at 695 cm^{-1} contains contributions from $^{10}BF_2{}^{37}Cl$ and $^{11}BF_2{}^{35}$-Cl, while the low-frequency component, at 691 cm^{-1}, is caused by $^{11}BF_2{}^{37}Cl$. The middle spectrum was recorded from a dilute solution in CH_3F, and the top spectrum was taken from a

solution containing a higher CH_3F concentration. New bands can be seen in these spectra at 686 and 682 cm^{-1}. Their relative intensity increases with the concentration of CH_3F, but so does the band at 691 cm^{-1}. Therefore, we assign complex bands at 691, 686, and 682 cm^{-1}, the former accidentally degenerate with the monomer band. Their assignment is complex, as can be inferred from the *ab initio* calculations, Tables 2 and 3, which show that the boron and chlorine isotopic splittings are compounded by conformational splittings: the transitions are predicted to be grouped in a quadruplet with a nearly constant frequency interval of 4 cm^{-1}, and with relative intensities, based on isotopic populations, close to 3, 16, 17, and 4. The relative intensities in Figure 3b then suggest that the three bands identified as due to the complex correspond to the lower three bands of the predicted quadruplet. This allows assignment of the 619-cm^{-1} band to the (^{10}B,^{35}Cl) isotope of the C_1 conformer and to the (^{10}B,^{37}Cl) and (^{11}B,^{35}Cl) isotopes of the C_s conformer. The band at 686 cm^{-1} is attributed to the (^{10}B,^{37}Cl) and ($^{11}B^{35}$-Cl) isotopes of C_1, and the ($^{11}B^{37}Cl$) isotope of C_s, while the band at 682 cm^{-1} must be due to the (^{11}B,^{37}Cl) isotope of the C_1 conformer.

Spectrum c in Figure 3 gives the region of ν_6^{BF2Cl}. The bottom spectrum was recorded from a solution containing only the boron halides. The band at 594 cm^{-1} is assigned to the ^{11}B monomer. The ^{10}B monomer band is expected near 620 cm^{-1}: this region is disturbed by an absorption band of the cell windows, and is not shown. The top spectrum was recorded from the same solution as Figure 1c. In agreement with this, the ^{11}B monomer band has all but disappeared, while the new bands at 587 and 560 cm^{-1} must be the $^{10}B/^{11}B$ isotopic doublet of ν_6^{BF2Cl} ($CH_3F{\cdot}BF_2Cl$).

The *ab initio* predictions also suggest that for ν_4^{BF2Cl} complex bands should be distinguishable. However, the spectra in this region are complicated by bands of $CH_3F{\cdot}BF_3$, $CH_3{\cdot}F$, and BCl_3, and no conclusive identification of all the bands in this region could be obtained.

Tables 4 and 5 suggest that not only for ν_1^{BFCl2} but also for a number of other fundamentals of $CH_3F{\cdot}BFCl_2$ complex bands should be observed. For this boron halide, unfortunately, circumstances are less favorable. In the first place, Figure 1c shows that at all times the bands of $CH_3F{\cdot}BFCl_2$ are very weak and, therefore, more difficult to observe. This is especially so for the CH stretch region, where the bands due to $CH_3F{\cdot}BFCl_2$ are predicted nearly degenerate with those of the substantially more concentrated $CH_3F{\cdot}BF_2Cl$. No complex bands could be detected for ν_4^{BFCl2} because they are overshadowed either by bands of $CH_3F{\cdot}BF_2Cl$ or by the extremily intense BCl_3 fundamentals just below 1000 cm^{-1}. The same is true for ν_3^{CH3F} ($CH_3F{\cdot}BFCl_2$), which occurs in the vicinity of the corresponding mode in the BF_2Cl complex. Because of its weakness, ν_2^{BFCl2} has not been identified in the monomer, let alone in the complex. Finally, ν_6^{BFCl2} in the monomer gives rise to weak bands at 541 and 519 cm^{-1}. The corresponding complex bands are predicted below 500 cm^{-1}. The signal-to-noise ratio in this region of the spectra is small due to the limited sensitivity of the MCT detector, while in this region ν_2^{BCl3} gives rise to absorptions. Therefore, no complex bands could be identified for this mode.

Altogether, it is clear that for $CH_3F{\cdot}BF_2Cl$ a substantial number of fundamentals has been detected. A clear indication for a conformational equilibrium is found only for ν_1^{BF2Cl}. This is not surprising, as the *ab initio* data, in combination with the spectral circumstances, suggest that only for this mode should an unambiguous conformational splitting be expected. Mostly due to experimental circumstances, for $CH_3F{\cdot}BFCl_2$ only the ν_1^{BFCl2} bands could be identified. Inevitably, the conformational splitting is observed only for this mode. However, the positions of the observed complex bands are in such close agreement with the *ab initio* predictions that the evidence for a conformational equilibrium is regarded as sufficiently convincing.

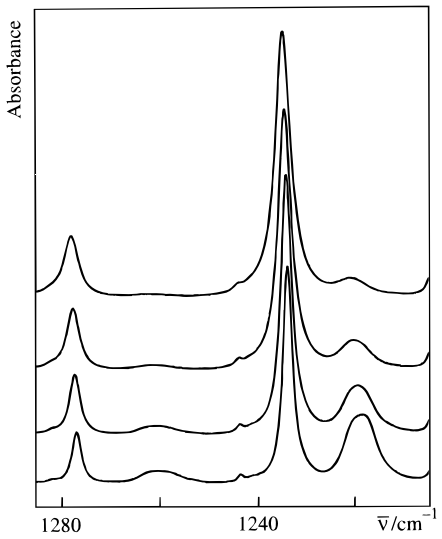

Figure 4. Infrared spectra of a solution in liquid argon, containing a mixture of boron trihalides and CH_3F, in the region of ν_1^{BF2Cl}. From top to bottom, the temperature of the solution decreases from 114.5 to 93.9 K.

The solutions, as indicated above, also contained BCl_3 in considerable excess. This compound gives rise[11] to very intense ν_3^{BCl3} multiplets near 985 and 950 cm^{-1}. The complexation lifts the degeneracy of this mode, with one complex band predicted at nearly the same frequency of the monomer mode, and the other, with similar intensity, red shifted by 15−20 cm^{-1}, the exact shift depending on the isotope. With the concentrations of BCl_3 obtained, the absorption in the fundamental ν_3 region is saturated over a fairly wide frequency region. Therefore, the chances of detecting the first complex band are nil. For $CH_3F{\cdot}^{10}BCl_3$ the second one is expected rather close to the monomer fundamental ν_3^{11BCl3}, and could be hidden under the latter. However, a complex band for $CH_3F{\cdot}^{11}BCl_3$, red shifted by 15−20 cm^{-1}, should in principle be detectable. In none of the spectra could a band attributable to this mode be detected. For the concentrations studied, ν_3^{BCl3} gives rise to well-defined first overtones, for which the complexation shifts should be approximately twice those of the fundamentals. Hence, in the region of the first overtones the complex bands should stand out more clearly. Close scrutinity of this region, however, also did not reveal the presence of complex bands. Therefore, we have to conclude that the concentration of $CH_3F{\cdot}BCl_3$ in the solutions investigated was below the detection limit. The spectra show that the concentrations of BCl_3 were substantially higher than those of BF_2Cl or $BFCl_2$, so the complex with BCl_3 must be significantly weaker. This is a very qualitative conclusion only, but it is an essential one when the order of Lewis acidity is to be considered.

The stability of the complexes, measured as the complexation enthalpy $\Delta H°$, was determined from a temperature study. The pronounced dependance of the relative intensity of the complex bands on temperature is illustrated in Figure 4 for ν_1^{BF2Cl}. Using band intensities I_i of species i from such spectra, the logarithm of $I_{CH_3F{\cdot}BF_xCl_y}/(I_{CH_3F} \times I_{BF_xCl_y})$ can be plotted against $1/T$. According the Van't Hoff isochore, the slope of the linear

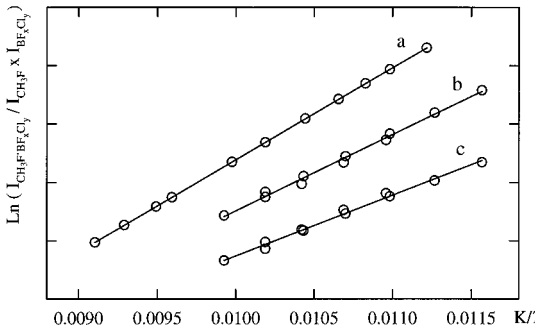

Figure 5. Van't Hoff plots for (a) $CH_3F{\cdot}BF_2Cl$, (b) the C_1 conformer, and (c) the C_s conformer of $CH_3F{\cdot}BFCl_2$.

regression line through the points of the plot, corrected for the thermal expansion of the solution,[12] equals $-\Delta H°/R$.

For $CH_3F{\cdot}BF_2Cl$, spectra were recorded between 92 and 117 K. Intensities I_{CH_3F} were obtained by numerical integration of $2\nu_3^{CH3F}$ between 2080 and 2050 cm^{-1}. The I_{BF_2Cl} and $I_{CH_3F{\cdot}BF_2Cl}$ were taken from band fitting of the $\nu_1^{11BF2Cl}$ region. In this analysis the contour of the complex band was represented by a doublet. The sum of these accurately reproduced the complex contour. Because of the strong overlap, however, the individual components were judged not to reliably represent the contributions of the C_1 and C_s conformers. Therefore, the sum intensity of the two components was used, leading to a complexation enthalpy averaged over the two conformers. The resulting Van't Hoff plot is shown in Figure 5a, and the $\Delta H°$ deduced from it equals $-12.4(3)$ kJ mol^{-1}.

For the $BFCl_2$ complexes, spectra were recorded between 86 and 98 K. The intensities I_{CH_3F} were obtained as for $CH_3F{\cdot}BF_2Cl$, while I_{BFCl_2} and $I_{CH_3F{\cdot}BFCl_2}$ were determined from a band fitting of the $\nu_1^{11BFCl2}$ region. The bands in this region are sufficiently separated, so that reliable intensities for each of the conformers, and for the monomer, were obtained. This allowed the construction of a Van't Hoff plot for each of the conformers. These are displayed in Figures 5, parts b and c. For the C_1 conformer a $\Delta H°$ of $-10.8(6)$ kJ mol^{-1} was calculated, and for the C_s conformer a value of $-8.6(6)$ kJ mol^{-1} was determined.

Discussion

The band fitting of the $\nu_1^{11BFCl2}$ region used in the derivation of $\Delta H°$ yields an integrated intensity for this mode in the C_1 conformer of $CH_3F{\cdot}BFCl_2$ which, at 86.6 K, is 7.9 times that for the C_s conformer. The *ab initio* calculations, Tables 4 and 5, suggest that both modes have very similar infrared intensities, so that the ratio of the integrated intensities measures the ratio of the populations of the conformers. The above intensity ratio, corrected for the 2-fold degeneracy of the C_1 conformer, is in agreement with the higher stability of the C_1 conformer found from the Van't Hoff plots, and from the *ab initio* calculations. Using a simple Boltzmann factor, the intensity ratio yields an energy difference of 1 kJ mol^{-1}, in acceptable agreement with the 1.74 kJ mol^{-1} obtained from the *ab initio* calculations, and with the difference between the complexation enthalpies in LAr of 2.2(6) kJ mol^{-1}.

A similar analysis allows the estimation of the relative stability of the conformers of $CH_3F{\cdot}BF_2Cl$. It was indicated above that for BF_2Cl the band fitting of the ν_1^{BF2Cl} region was judged unreliable, because of the very strong overlap of the components in the conformational doublets. The attempts at band fitting, however, indicate that, for instance at 89 K, the intensity of the low-frequency component of the conformational doublet is between 25% and 50% higher than that of the high-frequency component. This is, qualitatively, confirmed by the overall contours for the doublets in Figure 1. On the basis of the *ab initio* frequency predictions, the high-frequency component was assigned to the C_s conformer. The approximate intensity ratio, combined with the *ab initio* intensities from Tables 2 and 3, leads to conformer population ratios between 1.3 and 1.6, in favor of the C_1 conformer. When corrected for the 2-fold degeneracy of the latter, this result is compatible with the C_s conformer being the more stable, as predicted by the *ab initio* calculations, Table 1. A simple Boltzmann factor applied to the intensity ratios yields an energy difference between the conformers of 0.2 to 0.3 kJ mol^{-1}, whereas the *ab initio* result equals 0.48 kJ mol^{-1}.

The average $\Delta H°$ of $CH_3F{\cdot}BF_2Cl$ determined above, $-12.4(3)$ kJ mol^{-1}, is significantly smaller than that for the BF_3 complex,[3] $-16.8(5)$ kJ mol^{-1}, but is higher that that for the C_1 and C_s conformers of $CH_3F{\cdot}BFCl_2$, $-10.8(6)$ and $-8.6(6)$ kJ mol^{-1}, respectively. With the concentrations of BCl_3 used, the absence of bands due to a BCl_3 complex shows that $CH_3F{\cdot}BCl_3$ again must be weaker: from an estimate of relative intensities, and by neglecting entropy contributions, the $\Delta H°$ for the latter must be at least $2-3$ kJ mol^{-1} smaller than that for the C_s conformer of $CH_3F{\cdot}BFCl_2$. Thus, in liquid argon there is a systematic decrease of the stability of the complex with increasing chlorine content of the boron trihalide. For $CH_3F{\cdot}BF_3$, solvation energy calculations with the RHF-SCIPCM method[13] yield a solvent effect on the complexation enthalpy of 2.2 kJ mol^{-1}, putting the vapor phase complexation enthalpy at $-19.0(5)$ kJ mol^{-1}. Similar calculations for the compounds of this study are not available, so that the vapor phase complexation enthalpies for the present complexes cannot be extrapolated. For a qualitative estimate, it is instructive to compare the solvent stabilizations calculated with the above method[3] for BF_3 and CH_3F. The former has no dipole moment, while the value for the latter, calculated at the level used, is 2.16 D. In contrast with this difference in polarity, the stabilizations are calculated to be very similar, -3.7 kJ mol^{-1} for BF_3 and -3.0 kJ mol^{-1} for CH_3F. This is explained[13] by the fact that the polarizable continuum model uses the full solute's electron density distribution to calculate the solvent polarization. Moreover, the monomers, to a high degree, maintain their identity in the weak complexes, so that an increased solvent stabilization of one of the monomers is largely balanced by an increased stabilization of the complex. Therefore, the solvent effect on the complexation enthalpy is not expected to vary significantly from $CH_3F{\cdot}BF_3$ to $CH_3F{\cdot}BCl_3$. Hence, we may conclude that in the gas phase, the stability order of these complexes is the same as in liquid argon, i.e. the Lewis acidity of the boron halides decreases from BF_3 to BCl_3.

It remains now to explain the observed stability order. For a strong adduct between BX_3 and an electron donor, a covalent bond is formed by overlap of the free electron pair of the donor with the p_z orbital of the boron atom. The availability of the latter is a determining factor for the strength of the bond formed,[1] and, hence, for the Lewis acidity of BX_3. The availability, because of the π-back-bonding in the B−X bonds, decreases from X = F to X = Cl, so that for strong adducts the Lewis acidity of BCl_3 is found to exceed that of BF_3. For weak complexes involving the boron trihalides, the weakness is caused by the low tendency of the free electron pair of the electron donor to overlap with the boron p_z orbital. Hence, the bonding, as in most other van der Waals complexes,[14] is predominantly

(12) Van der Veken, B. J. *J. Phys. Chem.* **1996**, *100*, 17436.

(13) Foresman, J. B.; Keith, T. A.; Wiberg, K. B.; Snoonian, J.; Frisch, M. J. *J. Phys. Chem.* **1996**, *100*, 16098.

electrostatic. Then, the strength of the complex is not determined by the π-back-bonding, but by the electric charge on the boron atom. This charge, because of electroneagtivities, decreases with increasing substitution of F by Cl: this leads to the stability order observed in this study. This effect may be compounded by a sterical contribution due to the larger size of the chlorine atom. For strong adducts, the overlap with the boron p_z orbital causes a rehybridization of the boron atom, from sp^2 to sp^3. This causes the halogen susbstituents to bend away from the incoming Lewis base, thereby decreasing the sterical hindrance of bulkier chlorine substituents. However, for weak complexes the boron trihalide, as shown by the *ab initio* calculations, remains very nearly planar, so that more voluminous chlorine substituents on the boron atom prevent a close approach of the Lewis base, and this will contribute to the weakness of the bonding.

(14) Wales, D. J.; Popelier, P. L. A.; Stone, A. J. *J. Chem. Phys*. **1995**, *102*, 5551.

Acknowledgment. The Fund for Scientific Research (FWO, Belgium) is thanked for financial help toward the spectroscopic equipment used in this study. Support by the Flemish Community, through the Special Research Fund (BOF), is gratefully acknowledged.

JA9723850